INTERNATIONAL JOURNAL FOR NUMERICAL METHODS IN FLUIDS
Int. J. Numer. Meth. Fluids 2008; **56**:941–950
Published online 4 July 2007 in Wiley InterScience (www.interscience.wiley.com). DOI: 10.1002/fld.1566

Divergence-free discontinuous Galerkin schemes for the Stokes equations and the MAC scheme

Guido Kanschat*, †

Department of Mathematics, Texas A&M University, College Station, TX 77843-3368, U.S.A.

SUMMARY

We show that recently studied discontinuous Galerkin discretizations in their lowest order version are very similar to the marker and cell (MAC) finite difference scheme. Indeed, applying a slight modification, the exact MAC scheme can be recovered. Therefore, the analysis applied to the DG methods applies to the MAC scheme as well and the DG methods provide a natural generalization of the MAC scheme to higher order and irregular meshes. Copyright © 2007 John Wiley & Sons, Ltd.

Received 5 March 2007; Revised 30 May 2007; Accepted 30 May 2007

KEY WORDS: discontinuous Galerkin; divergence-free solutions; MAC scheme

1. INTRODUCTION

Divergence-conforming discontinuous Galerkin schemes recently suggested by Cockburn, Kanschat and Schötzau (see [1, 2], abbreviated as CKS below) generate pointwise divergence-free solutions to the incompressible Navier–Stokes equations without using a solenoidal basis; therefore, they are suitable for computations in three dimensions and on domains with complicated topology. While we were concerned with higher order approximations in [2], in this article it is shown that the version employing the lowest order Raviart–Thomas space on rectangular meshes is algebraically equivalent to the marker and cell (MAC) scheme of Harlow and Welch (see [3]).

The MAC scheme was introduced in 1965 as a stable finite difference scheme for incompressible flow problems. Nevertheless, its error analysis was presented only in 1992 (see [4, 5]) by transforming it to a finite volume scheme. Further results have been obtained by studying finite element methods yielding the same finite difference stencil. First, an analogy to mixed finite element methods for the vorticity–velocity–pressure formulation with divergence-conforming elements was

*Correspondence to: Guido Kanschat, Department of Mathematics, Texas A&M University, College Station, TX 77843-3368, U.S.A.
†E-mail: kanschat@tamu.edu

already found by Girault and Lopez (see [6]) in 1996. There, it was shown that the MAC scheme can be recovered by using a special numerical quadrature.

Han and Wu (see [7]) presented a finite element formulation of the MAC scheme using different staggered finite element meshes and obtained optimal energy error estimates for the velocity and pressure. Nevertheless, extension of this method to higher order elements suffers from the difficulty to handle three different meshes in two dimensions. Furthermore, a numerical quadrature rule is required to obtain the stencil of the MAC scheme.

The interest in the MAC scheme is to some extend due to the fact that it lends itself to the construction of efficient solvers for the discrete problem (see [8–11]). For that reason, a generalization of the MAC scheme to higher order and more general meshes is desirable.

Once the algebraic equivalence of the MAC scheme and the $H^{\mathrm{div}}(\Omega)$-conforming DG scheme is established, we exploit existing convergence results in order to derive estimates for the DG scheme. On the other hand, the DG scheme lends itself to the construction of higher order versions of the MAC scheme as well as the incorporation of locally refined meshes. Furthermore, it shows a way to interpolate solutions obtained by the MAC scheme to obtain a pointwise divergence-free function in $H^{\mathrm{div}}(\Omega)$.

In the remainder of this article, we first review the MAC scheme and the most important convergence result, followed by a description of the DG method. In Section 4, we show the equivalence of the two methods.

2. THE MAC SCHEME AND THE STAGGERED GRID

The MAC scheme as presented in [3] uses different, staggered grids for the pressure and each velocity component. In order to simplify the presentation, we assume the domain of computation is $\Omega = (0, 1)^2$ that the mesh consists of n^2 squares T_{ij} of size $h = 1/n$, numbered by index $i = 1, \ldots, n$ in the x-direction and $j = 1, \ldots, n$ in the y-direction. Note that the MAC scheme naturally extends to rectangular mesh cells and three-dimensional problems.

The distribution of degrees of freedom is shown in Figure 1. It shows the mesh cell T_{ij} with the pressure variable associated with the cell center and the velocity variables associated with the midpoints of the cell edges. We assign the coordinates $\mathbf{x}_{ij} = (t_i, t_j)^{\mathrm{T}}$ to the cell centers. Edge midpoints are offset in one direction and, therefore, are of the form $\mathbf{x}_{i-1/2,j} = (t_{i-1/2}, t_j)^{\mathrm{T}}$ and $\mathbf{x}_{i,j-1/2}$ for vertical and horizontal edges, respectively. The boundaries are at $t_{1/2} = 0$ and $t_{n+1/2} = 1$. The spacing is $t_{i+1} - t_i = h$. On this mesh, the gradient and divergence operators are discretized by

$$\partial_x^h p_{i+1/2,j} = \frac{1}{h}(p_{ij} - p_{i+1,j}) \tag{1}$$

$$\partial_y^h p_{i,j+1/2} = \frac{1}{h}(p_{ij} - p_{i,j+1}) \tag{2}$$

$$\nabla_h \cdot \mathbf{u}_{ij} = \frac{1}{h}(u_{i+1/2,j} - u_{i-1/2,j} + v_{i,j+1/2} - v_{i,j-1/2}) \tag{3}$$

We see that the gradient maps cell centers to edge midpoints and the divergence *vice versa*. The Laplacian of the velocity components in each point is approximated by the five-point stencil. For

DOI: 10.1002/fld

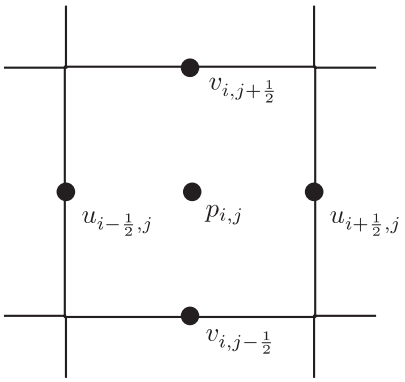

Figure 1. The placement of velocity and pressure values of the cell T_{ij} for the MAC scheme.

the velocity component u in the x-direction, this is

$$\begin{aligned} -\Delta^h u_{i+1/2,j} &= \partial^h_{xx} u_{i+1/2,j} + \partial^h_{yy} u_{i+1/2,j} \\ \partial^h_{xx} u_{i+1/2,j} &= \frac{2u_{i+1/2,j} - u_{i-1/2,j} - u_{i+3/2,j}}{h^2} \\ \partial^h_{yy} u_{i+1/2,j} &= \frac{2u_{i+1/2,j} - u_{i+1/2,j-1} - u_{i+1/2,j+1}}{h^2} \end{aligned} \tag{4}$$

The Laplacian of the velocity component v in the y-direction is defined accordingly. At the Dirichlet boundary, which coincides with the cell boundaries, the velocity nodes on the boundary are set to zero. This only affects the normal velocities.

While this scheme has been widely used in applications (see for example [12]), it took until [4] to obtain optimal error estimates for the vorticity and pressure. These were obtained by reinterpreting the MAC scheme in terms of the covolume method, thus employing suitable interpolations of the point values.

In [7], a finite element method related to the MAC scheme is presented. It uses separate rectangular finite element meshes for the variables u, v and p, respectively. It yields the optimal error estimates for u and p of the form

$$\|\nabla \mathbf{u} - \nabla \mathbf{u}_h\| + \|p - p_h\| = \mathcal{O}(h) \tag{5}$$

Remark 2.1

An error estimate for the velocities in L^2 follows from this results by standard duality arguments. This result also implies

$$\frac{1}{n}\sqrt{\sum_{ij}((u_{i+1/2,j} - u(t_{i+1/2}, t_j))^2 + (v_{i,j+1/2} - v(t_i, t_{j+1/2}))^2)} = \mathcal{O}(h^2) \tag{6}$$

on uniform meshes.

DOI: 10.1002/fld

Since the velocities are discretized by bilinear finite elements, a quadrature rule must be applied in order to obtain the five-point stencil of the MAC scheme. While this does not change the properties of the equation in an essential way, it makes devising higher order methods more difficult. Furthermore, *a posteriori* error estimates are more difficult to obtain.

3. THE DIVERGENCE-FREE DG METHOD

The discontinuous Galerkin discretizations of CKS type are based on $H^{\mathrm{div}}(\Omega)$-conforming finite elements for the velocity. They were analyzed in [1, 2] for higher order spaces. Here, we want to focus on the lowest order Raviart/Thomas space [13] RT_0 and its matching piecewise constant pressure space. In this space, the u-velocity is cellwise constant and discontinuous in the y-direction and cellwise linear and continuous in the x-direction. The v-velocity is *vice versa*.

Let us introduce the Lagrange interpolation polynomials on [0, 1] and $[t_{k-1/2}, t_{k+1/2}]$

$$\varphi^+(t) = t, \quad \varphi^-(t) = 1 - t$$

$$\varphi_k^+(t) = \varphi^+\left(\frac{t - t_{k-1/2}}{h}\right), \quad \varphi_k^-(t) = \varphi^-\left(\frac{t - t_{k-1/2}}{h}\right)$$

In order to ensure continuity of the normal component of the velocities over edges, we choose the values in edge midpoints as node values (see e.g. [14]). These are the support points for u and v of the MAC grid in Figure 1. Using the basis functions, the velocity on the cell T_{ij} has the form

$$\mathbf{u}_{ij}(x, y) = \begin{pmatrix} u_{i-1/2,j}\varphi_i^-(x) + u_{i+1/2,j}\varphi_i^+(x) \\ v_{i,j-1/2}\varphi_j^-(y) + u_{i,j+1/2}\varphi_j^+(y) \end{pmatrix} \tag{7}$$

for (x, y) in the mesh cell T_{ij}.

On the boundary, we enforce the condition $\mathbf{u} \cdot \mathbf{n} = 0$ strongly by restricting the finite element space (see [2]). The boundary condition on the tangential component will be enforced weakly in the momentum equation (10).

The discrete continuity equation is written in weak form as

$$b_h(\mathbf{u}, q) := \int_\Omega \nabla \cdot \mathbf{u}\, q \,\mathrm{d}x = 0 \quad \forall q \in Q_h \tag{8}$$

where Q_h is the space of cellwise constant pressure functions with mean value zero.

Integrating the form $b_h(\cdot, \cdot)$ by parts on each cell, we obtain the discrete gradient operator applied to p:

$$b_h(\Psi, p) = \sum_{T_{ij}} \left(-\int_{T_{ij}} \Psi \cdot \nabla p \,\mathrm{d}x + \int_{\partial T_{ij}} \Psi \cdot np \,\mathrm{d}x \right) = \sum_{E \in \mathscr{E}^{\mathrm{I}}} \int_E \Psi \cdot [\![pn]\!] \,\mathrm{d}x \tag{9}$$

where $\mathscr{E}^{\mathrm{I}}$ is the set of all interior edges.

It remains to consider the Laplacian in the momentum equation. In [2], feasibility of the CKS discretization for any stable consistent and self-adjoint DG scheme for the Laplacian is proven; even if we did not consider the case RT_0 there, the arguments are sufficiently abstract to extend to

DOI: 10.1002/fld

this case. Let us take the interior penalty method applied to each velocity component separately to start with. We choose $\Psi = (\psi, 0)^{\mathrm{T}}$.

$$\begin{aligned} a_h(\mathbf{u}, \Psi) = a_h(u, \psi) = \sum_{T_{ij}} \int_{T_{ij}} \nabla u \cdot \nabla \psi \, \mathrm{d}x + j_I(u, \psi) + j_D(u, \psi) \\ - \sum_{E \in \mathscr{E}^{\mathrm{I}}} \int_E (\{\{\nabla u\}\}[\![\psi \mathbf{n}]\!] + [\![u \mathbf{n}]\!]\{\{\nabla \psi\}\}) \, \mathrm{d}s \\ - \sum_{E \in \mathscr{E}^{\mathrm{D}}} (\psi \partial_{\mathbf{n}} u + u \partial_{\mathbf{n}} \psi) \, \mathrm{d}s \end{aligned} \tag{10}$$

where

$$j_I(u, \psi) = \sum_{E \in \mathscr{E}^{\mathrm{I}}} \frac{\kappa}{h_E} \int_E [\![u \mathbf{n}]\!][\![\psi \mathbf{n}]\!] \, \mathrm{d}s, \quad j_D(u, \psi) = \sum_{E \in \mathscr{E}^{\mathrm{D}}} 2 \frac{\kappa}{h_E} \int_E u \psi \, \mathrm{d}s \tag{11}$$

This method simplifies considerably in our case, since the normal components of the velocities are continuous, that is, $[\![u \mathbf{n}]\!] = 0$ and $[\![\psi \mathbf{n}]\!] = 0$ whenever $\mathbf{n}$ is parallel to the x-axis. Therefore, the jump terms only apply on edges parallel to the x-axis, where, on the other hand, the normal derivatives of u and ψ are zero. The same holds on the boundary due to the strong enforcement of $\mathbf{u} \cdot \mathbf{n} = 0$. Consequently,

$$a_h(u, \psi) = \sum_{T_{ij}} \int_{T_{ij}} \nabla u \cdot \nabla \psi \, \mathrm{d}\mathbf{x} + j_I(u, \psi) + j_D(u, \psi) \tag{12}$$

$$= \sum_{T_{ij}} \int_{T_{ij}} \nabla u \cdot \nabla \psi \, \mathrm{d}\mathbf{x} + j_I^x(u, \psi) + j_D^x(u, \psi) \tag{13}$$

where the superscript x on the second line indicates that the sum is restricted to edges parallel to the x-axis. In particular, since the indefinite part of the flux is missing, this bilinear form is stable for *all* positive values of κ (refer to, e.g. [15] or the proof for the modified form below).

4. THE STENCIL OF THE DG METHOD AND ITS RELATION TO THE MAC SCHEME

In this section, we compute the finite difference stencils associated with the discontinuous Galerkin method of the previous section. In order to do so, we compute rows of the resulting matrix by applying the bilinear forms to single basis functions as test functions.

4.1. Interior nodes

First, using the basis function q_{ij}, which is one on T_{ij} and zero elsewhere in the continuity Equation (8) yields

$$b_h(\mathbf{u}, q_{ij}) = \int_{T_{ij}} \nabla \cdot \mathbf{u} = h^2 \left(\frac{u_{i+1/2,j} - u_{i-1/2,j}}{h} + \frac{v_{i,j+1/2} - u_{i,j-1/2}}{h} \right) = h^2 \nabla_h \cdot u_{ij} \tag{14}$$

DOI: 10.1002/fld

Now, choose Ψ in (9) such that its first component is one at $x_{i+1/2,j}$ and zero in all other support points to obtain the discrete derivative of p in the x-direction from (9):

$$b_h(\Psi_{i+1/2,j},\, p) = h(p_{ij} - p_{i+1,j}) = h^2 \partial_x^h p_{i+1/2,j} \tag{15}$$

The same way, we obtain

$$b_h(\Psi_{i,j+1/2},\, p) = h(p_{ij} - p_{i,j+1}) = h^2 \partial_y^h p_{i,j+1/2} \tag{16}$$

Thus, the divergence and gradient operators of the DG method and the MAC scheme coincide up to a factor of h^2.

Let us now compute the stencil for the form $a_h(\cdot,\cdot)$ in (12) for the test function $\psi_{i+1/2,j}$ with support point $x_{i+1/2,j}$ and consider interior cells only:

$$\begin{aligned} a_h(u, \psi_{i+1/2,j}) = &\int_{T_{ij}} \frac{u_{i+1/2,j} - u_{i-1/2,j}}{h^2}\, \mathrm{d}\mathbf{x} - \int_{T_{i+1,j}} \frac{u_{i+3/2,j} - u_{i+1/2,j}}{h^2}\, \mathrm{d}\mathbf{x} \\ &+ \int_{x_{i+1/2}}^{x_{i+3/2}} \frac{\kappa}{h} (\partial_{yy}^h u_{i+3/2,j} \varphi_{i+1}^+(x) + \partial_{yy}^h u_{i+1/2,j} \varphi_{i+1}^-(x)) \varphi_{i+1}^-(x)\, \mathrm{d}x \\ &+ \int_{x_{i-1/2}}^{x_{i+1/2}} \frac{\kappa}{h} (\partial_{yy}^h u_{i+1/2,j} \varphi_i^+(x) + \partial_{yy}^h u_{i-1/2,j} \varphi_i^-(x)) \varphi_i^+(x)\, \mathrm{d}x \\ &= h^2 (\partial_{xx}^h u_{i+1/2,j} + \kappa \partial_{yy}^h u_{i+1/2,j} + \tfrac{\kappa}{6} \partial_{yy}^h u_{i-1/2,j} + \tfrac{\kappa}{6} \partial_{yy}^h u_{i+3/2,j}) \end{aligned} \tag{17}$$

This yields the difference stencil

$$\begin{bmatrix} -\frac{\kappa}{6} & -\kappa & -\frac{\kappa}{6} \\ \frac{\kappa}{3} - 1 & 2 + 2\kappa & \frac{\kappa}{3} - 1 \\ -\frac{\kappa}{6} & -\kappa & -\frac{\kappa}{6} \end{bmatrix}$$

We will now apply a modification to the edge terms of $a_h(\cdot,\cdot)$, such that the modified form is still stable, but the couplings to points offset diagonally vanish. To this end, we introduce the second-order Legendre polynomial on $[t_{i-1/2}, t_{i+1/2}]$, namely

$$\ell(t - t_{i-1/2}) = \frac{6h^2t^2 - 6ht + 1}{h}$$

and modify the jump term in (11) to

$$\tilde{j}_I(u, \psi) = \sum_{E \in \mathcal{E}^I} \frac{\kappa}{h_E} \int_E \frac{\gamma + \ell_E}{\gamma} [\![u\mathbf{n}]\!][\![\psi\mathbf{n}]\!]\, \mathrm{d}s \tag{18}$$

DOI: 10.1002/fld

where ℓ_E is the corresponding quadratic Legendre polynomial on the edge E. We choose γ to eliminate the cross coupling term:

$$\int_{t_{i-1/2}}^{t_{i+1/2}} \ell_E(t)\varphi_i^+(t)\varphi_i^-(t)\,\mathrm{d}t = h\int_0^1 (6t^2-6t+1)t(1-t)\,\mathrm{d}t = -\frac{h}{30}$$

$$\int_{t_{i-1/2}}^{t_{i+1/2}} \varphi_i^+(t)\varphi_i^-(t)\,\mathrm{d}t = \frac{h}{6}$$

Therefore, $\gamma = \frac{1}{5}$ yields

$$\int_{t_{i-1/2}}^{t_{i+1/2}} \frac{\gamma+\ell_E}{\gamma}\varphi^+(t)\varphi^-(t)\,\mathrm{d}t = 0 \tag{19}$$

The modified jump still defines a seminorm.

Lemma 4.1
The term

$$\tilde{j}_I^E = \int_E \frac{\gamma+\ell}{\gamma}[\![u\mathbf{n}]\!]^2\,\mathrm{d}s \tag{20}$$

is nonnegative and it is zero if and only if u is continuous along E.

Proof
The jump of u is linear functions along E and can be written as

$$[\![u(x)\mathbf{n}]\!] = a\varphi^+(x) + b\varphi^-(x)$$

with suitable coefficients a and b. Then,

$$\begin{aligned}\tilde{J}_I^E &= h\int_0^1 \frac{\gamma+\ell(t)}{\gamma}(a^2\varphi^+(t)^2 + b^2\varphi^-(t)^2 + 2ab\varphi^+(t)\varphi^-(t))\,\mathrm{d}t \\ &= h\int_0^1 \frac{\gamma+\ell(t)}{\gamma}(a^2\varphi^+(t)^2 + b^2\varphi^-(t)^2)\,\mathrm{d}t\end{aligned}$$

because of the choice of γ and ℓ. We have

$$\int_0^1 \ell(t)\varphi^+(t)^2\,\mathrm{d}t = \frac{1}{30} = \int_0^1 \ell(t)\varphi^-(t)^2\,\mathrm{d}t$$

Accordingly,

$$\tilde{j}_I^E = \frac{7h}{6}(a^2+b^2)$$

which is zero only if a and b are zero. □

DOI: 10.1002/fld

We introduce the modified boundary form

$$\tilde{j}_D(u,\psi) = 2 \sum_{E\in\mathscr{E}^D} \frac{\kappa}{h_E} \int_E \frac{\gamma+\ell}{\gamma} u\psi \,\mathrm{d}s \tag{21}$$

By the same means as in the proof to the previous lemma, we obtain that $\tilde{j}_D(u,u)=0$ if and only if $u=0$ on $\partial\Omega$. Therefore, we have the following lemma.

Lemma 4.2
The bilinear form

$$\tilde{a}_h(u,\psi) = \sum_{T_{ij}} \int_{T_{ij}} \nabla u \cdot \nabla\psi \,\mathrm{d}\mathbf{x} + \tilde{j}_I(u,\psi) + \tilde{j}_D(u,\psi) \tag{22}$$

is a positive definite, symmetric bilinear form on the space V_h with respect to the norm $\|\cdot\|_h = \sqrt{\tilde{a}_h(\cdot,\cdot)}$ for any $\kappa>0$.

Proof
Positive semi-definiteness and symmetry follow immediately from the definition of the form. The definiteness follows from the fact that if $\tilde{a}_h(u,u)=0$, the jump $j_I(u,u)$ enforces continuity, the boundary term $j_D(u,u)$ enforces homogeneous boundary conditions and the cell terms require that u is constant (for details see, e.g. [15]). □

Thus, the modified interior penalty formulation yields a stable DG finite element method with respect to the norm $\|\cdot\|_h = \sqrt{\tilde{a}_h(\cdot,\cdot)}$ and the analysis for the standard interior penalty method applies. Inserting expressions (20) and (19) for modified jumps into (17), we obtain the stencil

$$\begin{bmatrix} & -\frac{7}{6}\kappa & \\ -1 & 2+\frac{14}{6}\kappa & -1 \\ & -\frac{7}{6}\kappa & \end{bmatrix}$$

which for $\kappa=\frac{6}{7}$ yields the five-point stencil used in the original MAC scheme in [3].

4.2. Boundary conditions

In order to yield strongly divergence-free solutions, the CKS method requires that $\mathbf{u}\cdot\mathbf{n}=0$ on the boundary. This is nothing but the condition that the boundary nodes of the MAC scheme are set to zero.

The boundary condition for the tangential component is obtained in [3] by mirroring the value in the interior. Thus, we extend the mesh virtually by one layer of cells at each of the sides of the square. For instance, at the left boundary, we would add a layer of support points for v at $(t_0, t_{j-1/2})$ and let $v_{0,j-1/2} = -v_{1,j-1/2}$. Entering these values into the numerical flux (20) now yields exactly the boundary flux (21), which proves that the two formulations are algebraically equivalent at the boundary as well.

DOI: 10.1002/fld

5. CONVERGENCE OF THE LOWEST ORDER DG SCHEME

The convergence analysis of the CKS scheme involves standard energy error arguments in finite element analysis. A key ingredient there is an interpolation estimate of the form

$$\|\nabla \mathbf{u} - \nabla I_h \mathbf{u}\|_T \leqslant Ch^k \|\nabla^2 \mathbf{u}\|_T$$

where I_h is the interpolation operator into RT_k, h is the mesh size and k is the degree of the Raviart–Thomas element. This degree in our case is zero, such that this estimate is of no use. Even more, since the derivative of the RT_0 element in one space direction is always zero, no approximation in a norm involving the gradient can be achieved and, therefore, standard finite element convergence analysis fails.

Nevertheless, the interpolation estimate in L^2 reads

$$\|\mathbf{u} - I_h \mathbf{u}\|_T \leqslant Ch \|\nabla^2 \mathbf{u}\|_T \tag{23}$$

and we use it to obtain the following theorem.

Theorem 5.1
The solution obtained by the CKS method using lowest order Raviart–Thomas elements and piecewise constant pressures on uniform meshes admits the error estimates

$$\|\mathbf{u} - \mathbf{u}_h\| \leqslant Ch(\|\nabla^2 \mathbf{u}\| + \|\nabla p\|) \tag{24}$$

$$\|\mathbf{p} - \mathbf{p}_h\| \leqslant Ch(\|\nabla^2 \mathbf{u}\| + \|\nabla p\|) \tag{25}$$

Proof
We employ the fact that the CKS method is algebraically equivalent to the MAC scheme, and, therefore, to the finite element scheme by Han and Wu. Therefore, the solution u_{HW} coincides with u_h in the support points of the RT_0 element in Figure 1. Using the triangle inequality, we get

$$\|\mathbf{u} - \mathbf{u}_h\| \leqslant \|\mathbf{u} - I_h \mathbf{u}\| + \|I_h \mathbf{u} - I_h \mathbf{u}_{\mathrm{HW}}\| + \|I_h \mathbf{u}_{\mathrm{HW}} - \mathbf{u}_h\|$$

Here, the first term is estimated by the interpolation estimate (24). The last term vanishes, since the values of $\mathbf{u}_h$ and $\mathbf{u}_{\mathrm{HW}}$ coincide in the support points because of the equivalence of both schemes with the MAC scheme. The second term is of order h^2 by (6), taking into account that the support of all basis functions has the same size. Since the pressure space is the same as in [7], estimate (25) follows immediately their work. □

6. CONCLUSIONS

With a minor modification, we showed that the CKS scheme is algebraically equivalent to the MAC scheme. The modified scheme is still a consistent discontinuous Galerkin scheme. Therefore, it will enable us to develop *a posteriori* error estimates based on Galerkin orthogonality. Furthermore, it defines a pointwise divergence-free interpolation for the point values obtained by the MAC scheme. On the other hand, we could employ the convergence result for the MAC scheme to show first-order convergence of the lowest order CKS scheme. Finally, the CKS scheme in higher orders by the result in this article can be seen as a natural extension of the MAC scheme.

DOI: 10.1002/fld

REFERENCES

1. Cockburn B, Kanschat G, Schötzau D. A locally conservative LDG method for the incompressible Navier–Stokes equations. *Mathematics of Computation* 2005; **74**:1067–1095.
2. Cockburn B, Kanschat G, Schötzau D. A note on discontinuous Galerkin divergence-free solutions of the Navier–Stokes equations. *Journal of Scientific Computing* 2007; **31**:61–73.
3. Harlow FH, Welch JE. Numerical calculation of time-dependent viscous incompressible flow of fluid with free surface. *Physics of Fluids* 1965; **8**(12):2182–2189.
4. Nicolaides RA. Analysis and convergence of the MAC scheme. I. The linear problem. *SIAM Journal on Numerical Analysis* 1992; **29**(6):1579–1591.
5. Nicolaides RA, Wu X. Analysis and convergence of the MAC scheme. II. Navier–Stokes equations. *Mathematics of Computation* 1996; **65**(213):29–44.
6. Girault V, Lopez H. Finite-element error estimates for the MAC scheme. *IMA Journal of Numerical Analysis* 1996; **16**:347–379.
7. Han H, Wu X. A new mixed finite element formulation and the MAC method for the Stokes equations. *SIAM Journal on Numerical Analysis* 1998; **35**(2):560–571.
8. Elman HC. Multigrid and Krylov subspace methods for the discrete Stokes equations. *International Journal for Numerical Methods in Fluids* 1996; **22**(8):755–770.
9. Elman HC. Preconditioning for the steady-state Navier–Stokes equations with low viscosity. *SIAM Journal on Scientific Computing* 1999; **20**(4):1299–1316.
10. Wittum G. Multi-grid methods for Stokes and Navier–Stokes equations. Transforming smoothers: algorithms and numerical results. *Numerische Mathematik* 1989; **54**(5):543–563.
11. Wittum G. On the convergence of multi-grid methods with transforming smoothers. Theory with applications to the Navier–Stokes equations. *Numerische Mathematik* 1990; **57**(1):15–38.
12. Zienkiewicz OC, Taylor RL, Nithiarasu P. *The Finite Element Method for Fluid Dynamics*. Elsevier: Amsterdam, 2005.
13. Raviart P-A, Thomas JM. A mixed method for second order elliptic problems. In *Mathematical Aspects of the Finite Element Method*, Galligani I, Magenes E (eds). Springer: New York, 1977.
14. Brezzi F, Fortin M. *Mixed and Hybrid Finite Element Methods*. Springer: Berlin, 1991.
15. Kanschat G. Discontinuous Galerkin Methods for Viscous Flow. *Habilitation Thesis*, Heidelberg, 2004.

DOI: 10.1002/fld